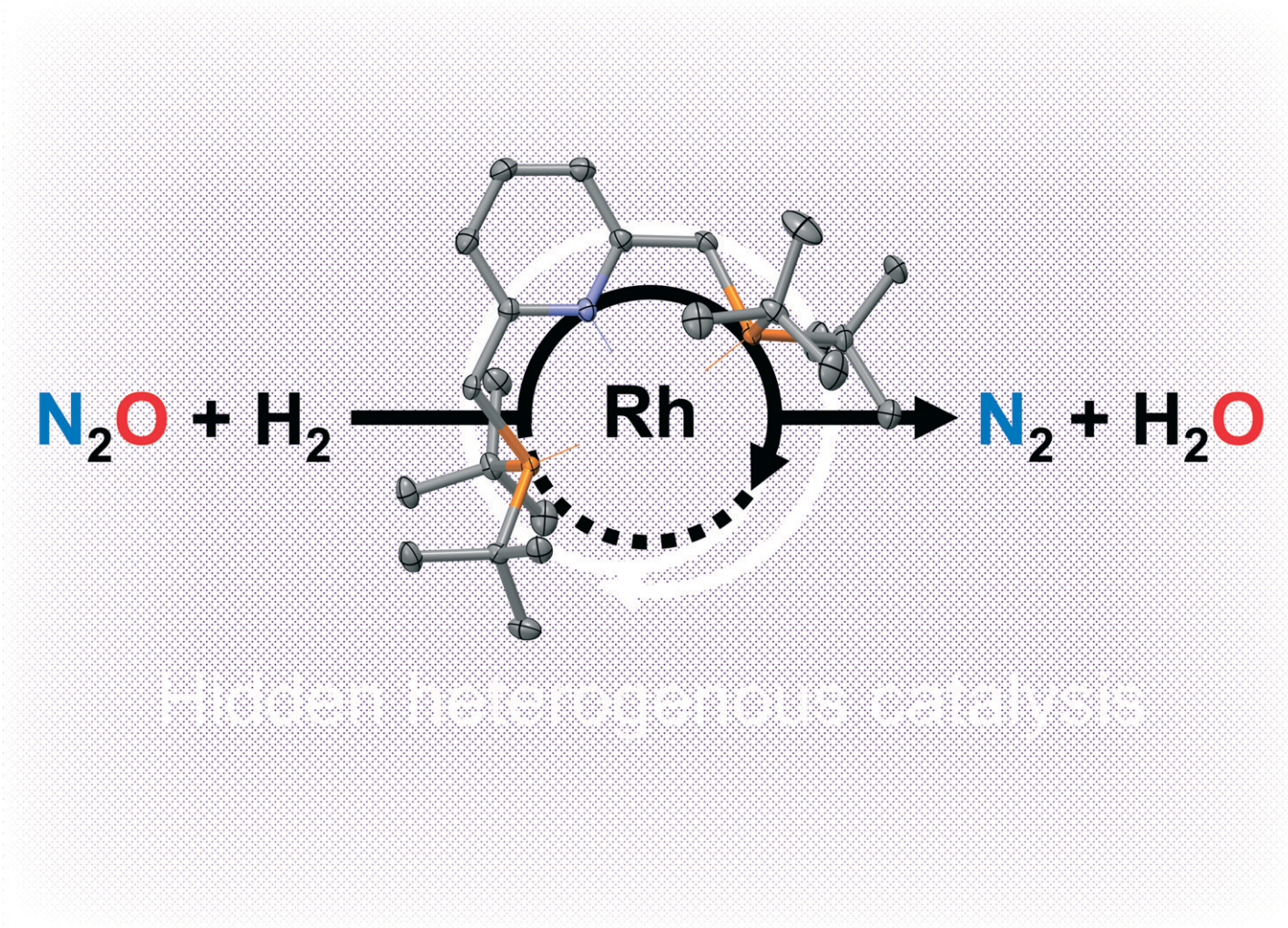

Showcasing research from the University of Warwick, UK.

Rhodium-catalysed hydrogenation of nitrous oxide

The hydrogenation of nitrous oxide is a thermodynamically favourable transformation relevant to the remediation of this potent greenhouse gas and ozone-depleting substance. Few homogeneous catalysts can operate under the aggressive reaction conditions involved, and our work highlights the potential for molecular complexes of platinum-group metals to decompose into catalytically active nanoparticles.

Image reproduced by permission of Adrian Chaplin from *Catal. Sci. Technol.*, 2025, **15**, 4126.

As featured in:

See Adrian B. Chaplin *et al.*, *Catal. Sci. Technol.*, 2025, **15**, 4126.

ROYAL SOCIETY OF CHEMISTRY

rsc.li/catalysis

Registered charity number: 207890

Catalysis Science & Technology

ROYAL SOCIETY OF CHEMISTRY

COMMUNICATION

View Article Online
View Journal | View Issue

Cite this: *Catal. Sci. Technol.*, 2025, **15**, 4126

Received 23rd April 2025,
Accepted 17th June 2025

DOI: 10.1039/d5cy00490j

rsc.li/catalysis

Rhodium-catalysed hydrogenation of nitrous oxide†

Sophie H. Dewick,[a] Thomas M. Hood,[a] Yisong Han,[b] Steven Huband[b] and Adrian B. Chaplin*[a]

We report on the discovery of "hidden" heterogeneous catalysis in the hydrogenation of nitrous oxide while assessing the catalytic activity of a rhodium(I) hydride complex supported by a nominally robust phosphine-based pincer ligand. Commercially available $[Rh(COD)(OH)]_2$ was subsequently identified as a more effective catalyst precursor, enabling the hydrogenation of nitrous oxide with an apparent turnover number >3000 at room temeprature.

Nitrous oxide (N_2O) is a long-lived gas that accumulates in the atmosphere, contributing to climate change as a potent greenhouse gas and leading to ozone depletion in the stratosphere.[1] Although chemical activation is challenging, exponentially increasing anthropogenic emissions of N_2O make it imperative that energy efficient methods are developed to remediate point sources of this atmospheric pollutant.[2] Direct decomposition into N_2 and O_2 is encumbered by the formidable kinetic stability of N_2O, necessitating temperatures >700 °C at atmospheric pressure.[3] While heterogeneous catalysts can promote this reaction (*ca.* 300–600 °C), variants where sacrificial reducing agents are added to facilitate removal of surface oxygen atoms are capable of operating at lower temperatures and more appealing from a remediation perspective.[4] In this context, the hydrogenation of N_2O to afford N_2 and H_2O is a thermodynamically favourable, yet undeveloped transformation, using either heterogeneous or homogeneous catalysts.

Of the limited examples of heterogeneous N_2O hydrogenation described in the literature,[5] the use of platinum group metal catalysts is outstanding for the mild operating temperatures involved. For instance, ruthenium, rhodium, palladium, and platinum supported on titania promote the hydrogenation of N_2O between 50–150 °C, with activity increasing in the order Pd > Rh > Pt > Ru based on measurements made using a flow reactor.[6] Rhodium supported on SiO_2 and Al_2O_3 is also active under flow conditions and a TOF of 0.022 s^{-1} was measured for the former at 72 °C.[7] Molecular complexes of the platinum group metals have additionally been investigated as homogeneous catalysts, with seminal work using ruthenium pincer complexes reported by Milstein in 2017 (Fig. 1).[8] A mechanism involving O-atom insertion into a Ru–H bond, coupled with bifunctional reactivity of the supporting PNP pincer ligand, was proposed and 417 TONs achieved over 48 h at 65 °C. More productive catalysts have since been identified,[9,10] including a remarkable rhodium-based system by Trincado and Grützmacher, during the preparation of this manuscript, which delivered 230 000 apparent TONs after 96 h at 65 °C (Fig. 1).[11]

Building upon our work with rhodium pincer complexes, which has included the isolation of well-defined Rh–N_2O adducts,[12] we became interested in assessing the relative catalytic activity of the homologous series of complexes **1–3**

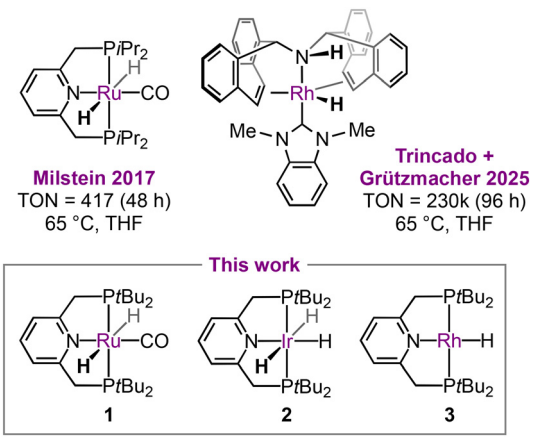

Fig. 1 Late transition metal hydride complexes used as catalysts for the hydrogenation of nitrous oxide.

[a] *Department of Chemistry, University of Warwick, Coventry CV4 7AL, UK. E-mail: a.b.chaplin@warwick.ac.uk*
[b] *Department of Physics, University of Warwick, Coventry CV4 7AL, UK*

† Electronic supplementary information (ESI) available: Full experimental details, including analysis of catalytic reactions and characterisation of rhodium nanoparticles by TEM/EDX and SAXS. See DOI: https://doi.org/10.1039/d5cy00490j

Table 1 Catalyst screening for the hydrogenation of N_2O[a]

Entry	Catalyst (additive/variation)	$[H_2O]$/M	TON
1	None	0.00	—
2	[Ru(PNP-*t*Bu)HCl(CO)] (+KO*t*Bu)[b]	0.03	5
3	[Ir(PNP-*t*Bu)H_3] **2**	0.01	1
4	[Rh(PNP-*t*Bu)H] **3**[c]	0.90	174
5	[Rh(PNP-*t*Bu)H] **3** (+Hg)	0.01	2
6	[Rh(PNP-*t*Bu)H] **3** (THF→CyH)	<0.01	<1
7	[Rh(PNP-*t*Bu)(OH)] **4**[c]	0.75	146
8	[Rh(PNP*-*t*Bu)N_2] **5**[c]	0.75	144
9	Rh/C[d]	0.24	47
10	$[Rh(COD)(OH)]_2$ **6**[c]	1.72	318
11	$[Rh(COD)(OH)]_2$ **6** (t = 1 h)[c]	0.03	6

[a] Conditions: 10 μmol of catalyst/Rh in 2.0 mL of THF placed under ~1 : 2 H_2/N_2O (3 atm) within a 100 mL gas bulb with cold finger (126 mL water volume) and stirred at RT for 24 h. Conversion determined by ^{1}H NMR analysis using a mesitylene internal standard and averaged over duplicate runs. [b] No conversion observed in the absence of KO*t*Bu. [c] Generation of N_2 verified by head space analysis (GC-TCD). [d] Hydrogenation of the internal standard was observed. Similar activity is achieved in the absence of the internal standard.

(Fig. 1). Octahedral hydride complexes **1** (generated from [Ru(PNP-*t*Bu)(CO)HCl] and KO*t*Bu) and **2** have previously been assessed by Milstein and Suárez,[8,9] and we hypothesised that the component phosphine-based pincer ligand PNP-*t*Bu would be a thermally robust scaffold that would support the homogeneous hydrogenation of N_2O using square-planar rhodium(I) hydride **3**.[13,14]

The hydrogenation of N_2O was first examined at RT using 5 mM solutions of **1**–**3** in 2.0 mL THF, stirred within the cold finger of a 100 mL gas bulb pressurised with a ~1 : 2 mixture of H_2/N_2O (3 atm, Table 1). Under these net oxidising conditions, **1** and **2** showed very low catalytic activity, whereas **3** gave 174 apparent TONs over 24 h: as quantified by the formation of water by ^{1}H NMR spectroscopy with the generation of N_2 verified by GC-TCD analysis of the head space.

Encouraged by the high catalytic activity of **3**, we sought to understand the underlying mechanism. To this end, the reaction between **3** (20 mM) and N_2O (2 atm) was examined *in situ* by NMR spectroscopy in d^8-THF, revealing quantitative spectroscopic conversion of **3** into a ~1 : 1 mixture of the known rhodium(I) hydroxide complex **4** (δ_{31P} 55.6, $^1J_{RhP}$ = 162 Hz) and dearomatized rhodium(I) dinitrogen complex **5** (δ_{31P} 66.6, $^1J_{RhP}$ = 132 Hz; 63.1, $^1J_{RhP}$ = 132 Hz; $^2J_{PP}$ = 269 Hz) within 5 min at RT (Scheme 1).[15] This outcome is consistent with activation of N_2O by O-atom insertion into the Rh–H bond,[16] followed by (partial) bifunctional elimination of water as proposed for **1** by Milstein.[8] Although independently isolated **4** and **5** are catalytically competent for the hydrogenation of N_2O under the aforementioned conditions (Table 1), they react incompatibly slowly with H_2 at RT on a NMR reaction scale and, moreover, do not reform **3** cleanly (Scheme 1). Likewise, whilst **4** eliminated water to give **5** under an atmosphere of N_2 and treatment of **5** with excess water gave

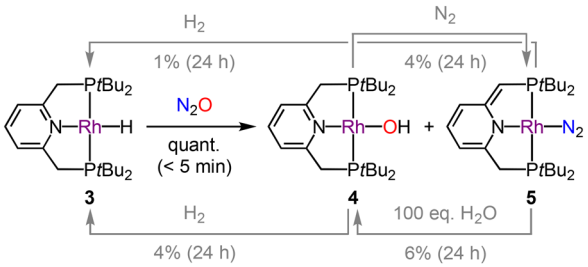

Scheme 1 Reactions of isolated **1**–**3** in d^8-THF at RT.

4, both reactions are sluggish at RT and partial decomposition was observed during the former. This decomposition is attributed to the instability of **5** and a significant amount of PNP-*t*Bu oxide was produced when a 20 mM solution of **5** in d^8-THF was placed under N_2O (2 atm; 11% after 24 h at RT by ^{31}P NMR spectroscopy). No reaction with **4** was observed under the same conditions.

These observations, coupled with the deposition of dark residues on the reactor walls and observation of PNP-*t*Bu oxide by ^{31}P NMR spectroscopy when using **3** in catalysis, led us to question the homogeneous nature of the hydrogenation. The formation of 2.9 ± 0.4 nm rhodium nanoparticles was subsequently confirmed by TEM/EDX analysis of the post-catalysis reaction mixture (Fig. 2A), and their role in catalysis corroborated by a positive mercury drop test, in which addition of mercury almost completely inhibited catalysis using **3** (Table 1, entry 5).[17] The N_2O hydrogenation observed for **3** is therefore not attributed to homogeneous catalysis as we hypothesized, but instead reconciled by the formation of catalytically-active rhodium nanoparticles from partial decomposition of **5** under the reaction conditions (generated from **3** + N_2O or **4** − H_2O, Scheme 1). Isolated **5** displays significantly enhanced stability in cyclohexane and, in further support of this conclusion, **3** is an ineffective catalyst for N_2O hydrogenation when cyclohexane is used in place of THF as the reaction solvent (Table 1, entry 6).

Having concluded that **3** operates *via* heterogeneous catalysis, we sought to identify a more convenient source of rhodium to apply in the hydrogenation of N_2O (Table 1). Commercially available Rh/C was first assessed under our conditions but gave only 47 apparent TONs over 24 h. The use of bench stable $[Rh(COD)(OH)]_2$ (**6**, COD = 1,5-cyclooctadiene) as a nanoparticle precursor was more promising,[18] with a catalytic turnover nearly double that of **3** recorded after 24 h. Disproportionately low turnover after 1 h is symptomatic of an induction period for **6** and post catalysis analysis of the different runs by SAXS suggests that activity may correlate with a greater degree of nanoparticle aggregation. For instance, particles of mean radius 26.6 nm were observed after 1 h, while after 24 h the scattering data are best modelled as a mixture containing particles with a mean radius of 58.6 nm (see ESI†). These changes in aggregation are also apparent from TEM/EDX analysis of the samples (Fig. 2B/C).

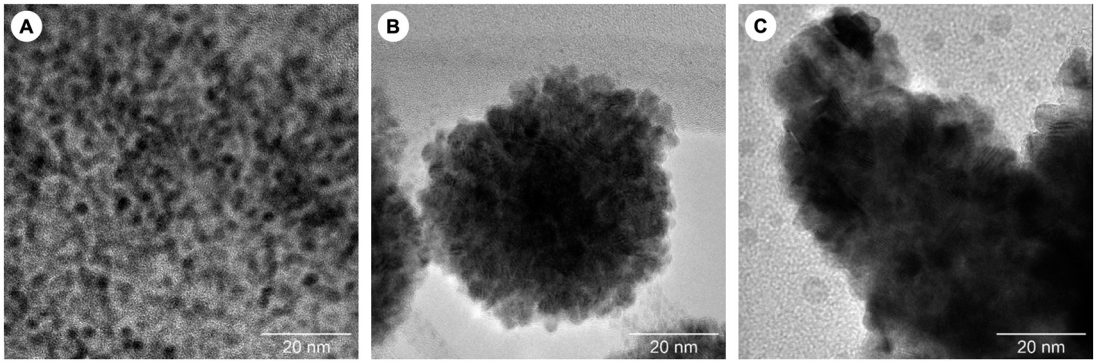

Fig. 2 TEM images taken from post catalysis reaction mixtures when using (A) **3**, (B) **6** (1 h run) and (C) **6** (24 h run).

To further explore the catalytic utility of **6**, the hydrogenation reaction was tested on a larger scale using a 250 mL gas bulb, under otherwise unoptimised reaction conditions: 5 mM $[Rh(COD)(OH)]_2$ in 2.0 mL of THF, ~1 : 2 H_2/N_2O (3 atm). After three successive 24 h cycles, where average cumulative apparent TONs of 982, 2055 and 3261 were measured, a total of 16.3 M of water was produced.

In summary, we have discovered "hidden" heterogenous catalysis in the hydrogenation of N_2O using a rhodium(I) hydride complex featuring a nominally robust phosphine-based pincer ligand. Although reaction with N_2O by O-atom insertion into the Rh–H bond is facile, the ensuing dearomatized rhodium(I) derivative is unstable and partial decomposition into catalytically active rhodium nanoparticles and PNP-*t*Bu oxide was observed during catalysis. Commercially available and bench stable $[Rh(COD)(OH)]_2$ was identified as a more effective catalyst precursor, enabling the hydrogenation of N_2O with an apparent turnover number >3000 at RT. We encourage the possible formation of small quantities of catalytically active nanoparticles to be carefully assessed when using molecular catalysts for this reaction.

Data availability

The data supporting this article have been included as part of the ESI.†[19]

Conflicts of interest

There are no conflicts to declare.

Acknowledgements

This work was supported by NERC grants NE/S007350/1 (CENTA2 studentship to SHD) and NE/X018377/1. We also acknowledge funding from the Leverhulme Trust (RPG-2022-214, TMH) and the University of Warwick. TEM and SAXS measurements were made using equipment provided by the University of Warwick Electron Microscopy and X-ray Diffraction Research Technology Platforms.

Notes and references

1 (*a*) *Climate Change 2023: Synthesis Report*, ed. H. Lee and J. Romero, Intergovernmental Panel on Climate Change, Geneva, Switzerland, 2023, DOI: **10.59327/ipcc/ar6-9789291691647**; (*b*) A. R. Ravishankara, J. S. Daniel and R. W. Portmann, *Science*, 2009, **326**, 123–125.

2 H. Tian, R. Xu, J. G. Canadell, R. L. Thompson, W. Winiwarter, P. Suntharalingam, E. A. Davidson, P. Ciais, R. B. Jackson, G. Janssens-Maenhout, M. J. Prather, P. Regnier, N. Pan, S. Pan, G. P. Peters, H. Shi, F. N. Tubiello, S. Zaehle, F. Zhou, A. Arneth, G. Battaglia, S. Berthet, L. Bopp, A. F. Bouwman, E. T. Buitenhuis, J. Chang, M. P. Chipperfield, S. R. S. Dangal, E. Dlugokencky, J. W. Elkins, B. D. Eyre, B. Fu, B. Hall, A. Ito, F. Joos, P. B. Krummel, A. Landolfi, G. G. Laruelle, R. Lauerwald, W. Li, S. Lienert, T. Maavara, M. MacLeod, D. B. Millet, S. Olin, P. K. Patra, R. G. Prinn, P. A. Raymond, D. J. Ruiz, G. R. van der Werf, N. Vuichard, J. Wang, R. F. Weiss, K. C. Wells, C. Wilson, J. Yang and Y. Yao, *Nature*, 2020, **586**, 248–256.

3 P. Glarborg, J. E. Johnsson and K. Dam-Johansen, *Combust. Flame*, 1994, **99**, 523–532.

4 X. Wu, J. Du, Y. Gao, H. Wang, C. Zhang, R. Zhang, H. He, G. M. Lu and Z. Wu, *Chem. Soc. Rev.*, 2024, **53**, 8379–8423.

5 (*a*) L. Jacobs, C. Barroo, N. Gilis, S. V. Lambeets, E. Genty and T. V. de Bocarmé, *Appl. Surf. Sci.*, 2018, **435**, 914–919; (*b*) J. Arenas-Alatorre, A. Gómez-Cortés, M. Avalos-Borja and G. Díaz, *J. Phys. Chem. B*, 2005, **109**, 2371–2376; (*c*) T. Nobukawa, M. Yoshida, K. Okumura, K. Tomishige and K. Kunimori, *J. Catal.*, 2005, **229**, 374–388; (*d*) A. C. Gluhoi, M. A. P. Dekkers and B. E. Nieuwenhuys, *J. Catal.*, 2003, **219**, 197–205; (*e*) G. Delahay, M. Mauvezin, A. Guzmán-Vargas and B. Coq, *Catal. Commun.*, 2002, **3**, 385–389; (*f*) S. A. Carabineiro and B. E. Nieuwenhuys, *Surf. Sci.*, 2001, **495**, 1–7; (*g*) A. Dandekar and M. A. Vannice, *Appl. Catal., B*, 1999, **22**, 179–200; (*h*) J. E. Vance and J. K. Dixon, *J. Am. Chem. Soc.*, 1941, **63**, 176–181; (*i*) J. K. Dixon and J. E. Vance, *J. Am. Chem. Soc.*, 1935, **57**, 818–821; (*j*) A. F. Benton and C. M. Thacker, *J. Am. Chem. Soc.*, 1934, **56**, 1300–1304; (*k*) H. Cassel and E. Glückauf, *Z. Phys. Chem.*,

Abt. B, 1932, **19**, 47–62; (*l*) C. N. Hinshelwood, *Proc. R. Soc. London, Ser. A*, 1924, **106**, 292–298.

6 S. Roy, M. S. Hegde, S. Sharma, N. P. Lalla, A. Marimuthu and G. Madras, *Appl. Catal., B*, 2008, **84**, 341–350.

7 (*a*) N. W. Cant, D. C. Chambers and I. O. Y. Liu, *J. Catal.*, 2011, **278**, 162–166; (*b*) A. Miyamoto, S. Baba, M. Mori and Y. Murakami, *J. Phys. Chem.*, 1981, **85**, 3117–3122.

8 R. Zeng, M. Feller, Y. Ben-David and D. Milstein, *J. Am. Chem. Soc.*, 2017, **139**, 5720–5723.

9 I. Ortega-Lepe, P. Sánchez, L. L. Santos, P. Lara, N. Rendón, J. López-Serrano, V. Salazar-Pereda, E. Álvarez, M. Paneque and A. Suárez, *Inorg. Chem.*, 2022, **61**, 18590–18600.

10 P. Jurt, A. S. Abels, J. J. Gamboa-Carballo, I. Fernández, G. L. Corre, M. Aebli, M. G. Baker, F. Eiler, F. Müller, M. Wörle, R. Verel, S. Gauthier, M. Trincado, T. L. Gianetti and H. Grützmacher, *Angew. Chem., Int. Ed.*, 2021, **60**, 25372–25380.

11 S. T. Nappen, J. J. Gamboa-Carballo, E. Tschanen, F. Ricatto, M. D. Wörle, A. Thomas, M. Trincado and H. Grützmacher, *Angew. Chem., Int. Ed.*, 2025, **64**, e202502616.

12 M. R. Gyton, B. Leforestier and A. B. Chaplin, *Angew. Chem., Int. Ed.*, 2019, **58**, 15295–15298.

13 L. Schwartsburd, M. A. Iron, L. Konstantinovski, E. Ben-Ari and D. Milstein, *Organometallics*, 2011, **30**, 2721–2729.

14 E. Peris and R. H. Crabtree, *Chem. Soc. Rev.*, 2018, **47**, 1959–1968.

15 (*a*) S. K. Hanson, D. M. Heinekey and K. I. Goldberg, *Organometallics*, 2008, **27**, 1454–1463; (*b*) S. M. Kloek, D. M. Heinekey and K. I. Goldberg, *Angew. Chem., Int. Ed.*, 2007, **46**, 4736–4738.

16 (*a*) T. L. Gianetti, S. P. Annen, G. Santiso-Quinones, M. Reiher, M. Driess and H. Grützmacher, *Angew. Chem., Int. Ed.*, 2016, **55**, 1854–1858; (*b*) J.-H. Lee, M. Pink, J. Tomaszewski, H. Fan and K. G. Caulton, *J. Am. Chem. Soc.*, 2007, **129**, 8706–8707; (*c*) A. W. Kaplan and R. G. Bergman, *Organometallics*, 1998, **17**, 5072–5085; (*d*) A. W. Kaplan and R. G. Bergman, *Organometallics*, 1997, **16**, 1106–1108.

17 (*a*) R. H. Crabtree, *Chem. Rev.*, 2012, **112**, 1536–1554; (*b*) J. A. Widegren and R. G. Finke, *J. Mol. Catal. A: Chem.*, 2003, **198**, 317–341.

18 D.-H. Liu, P. M. Pflüger, A. Outlaw, L. Lückemeier, F. Zhang, C. Regan, H. R. Nodeh, T. Cernak, J. Ma and F. Glorius, *J. Am. Chem. Soc.*, 2024, **146**, 11866–11875.

19 (*a*) S. D. Pike, M. R. Crimmin and A. B. Chaplin, *Chem. Commun.*, 2017, **53**, 3615–3633; (*b*) B. Gnanaprakasam, J. Zhang and D. Milstein, *Angew. Chem., Int. Ed.*, 2010, **49**, 1468–1471; (*c*) A. van der Ent, A. L. Onderdelinden and R. A. Schunn, *Inorg. Synth.*, 1990, **28**, 90–92; (*d*) D. Hermann, M. Gandelman, H. Rozenberg, L. J. W. Shimon and D. Milstein, *Organometallics*, 2002, **21**, 812–818; (*e*) M. R. Gyton, T. M. Hood and A. B. Chaplin, *Dalton Trans.*, 2019, **48**, 2877–2880; (*f*) E. M. Pelczar, T. J. Emge, K. Krogh-Jespersen and A. S. Goldman, *Organometallics*, 2008, **27**, 5759–5767; (*g*) R. Uson, L. A. Oro, J. A. Cabeza, H. E. Bryndza and M. P. Stepro, *Inorg. Synth.*, 1985, **23**, 126–130; (*h*) P. S. Pregosin, *NMR in Organometallic Chemistry*, Wiley-VCH, 2012, pp. 251–254; (*i*) *XSACT: X-ray scattering, analysis, and calculation tool (Xenocs, version 2.7)*, 2023; (*j*) J. Ilavsky and P. R. Jemian, *J. Appl. Crystallogr.*, 2009, **42**, 347–353; (*k*) W. Li, J.-H. Xie, H. Lin and Q.-L. Zhou, *Green Chem.*, 2012, **14**, 2388–2390; (*l*) L. R. Doyle, A. Heath, C. H. Low and A. E. Ashley, *Adv. Synth. Catal.*, 2014, **356**, 603–608.